

# CDR1as regulates $\alpha$ -synuclein-mediated ischemic brain damage by controlling miR-7 availability

Suresh L. Mehta,<sup>1</sup> Anil K. Chokkalla,<sup>1</sup> Saivenkateshkomal Bathula,<sup>1</sup> Vijay Arruri,<sup>1</sup> Bharath Chelluboina,<sup>1</sup> and Raghu Vemuganti<sup>1,2</sup>

<sup>1</sup>Department of Neurological Surgery, University of Wisconsin-Madison, Madison, WI 53792, USA; <sup>2</sup>William S. Middleton Veterans Administration Hospital, Madison, WI 53792, USA

**Transient focal ischemia decreased microRNA-7 (miR-7) levels, leading to derepression of its major target  $\alpha$ -synuclein ( $\alpha$ -Syn) that promotes secondary brain damage. Circular RNA CDR1as is known to regulate miR-7 abundance and function. Hence, we currently evaluated its functional significance after focal ischemia. Transient middle cerebral artery occlusion (MCAO) in adult mice significantly downregulated both CDR1as and miR-7 levels in the peri-infarct cortex between 3 and 72 h of reperfusion. Interestingly, neither pri-miR-7a nor 7b was altered in the ischemic brain. Intracerebral injection of an AAV9 vector containing a CDR1as gene significantly increased CDR1as levels by 21 days that persisted up to 4 months without inducing any observable toxicity in both sham and MCAO groups. Following transient MCAO, there was a significant increase in miR-7 levels and CDR1as binding to Ago2/miR-7 in the peri-infarct cortex of AAV9-CDR1as cohort compared with AAV9-Control cohort at 1 day of reperfusion. CDR1as overexpression significantly suppressed post-stroke  $\alpha$ -Syn protein induction, promoted motor function recovery, decreased infarct size, and curtailed the markers of apoptosis, autophagy mitochondrial fragmentation, and inflammation in the post-stroke brain compared with AAV9-Control-treated cohort. Overall, our findings imply that CDR1as reconstitution is neuroprotective after stroke, probably by protecting miR-7 and preventing  $\alpha$ -Syn-mediated neuronal death.**

## INTRODUCTION

Focal cerebral ischemia rapidly alters the expression of several classes of noncoding RNAs (ncRNAs), including circular RNAs (circRNAs), microRNAs (miRNAs), and long ncRNAs (lncRNAs).<sup>1-4</sup> They can affect the post-ischemic functional outcome by influencing chromatin architecture, RNA/protein scaffolding, enhancer function, alternative splicing, RNA stability, transcription, and translation.<sup>5-10</sup> The ncRNAs regulate each other, which is critical for their functionality and stability in the cellular milieu.<sup>11-13</sup> The circRNAs formed by back-splicing and covalent linkage of the 5' and 3' ends are resistant to exonucleases that digest linear RNAs. Many circRNAs sponge miRNAs or proteins and thus modulate transcription and translation.<sup>8</sup>

The cerebellar degeneration-related protein 1 antisense RNA (CDR1as), also known as the circular RNA sponge for miR-7 (ciRS-7), is a neurally abundant and conserved circRNA in mammals.<sup>14,15</sup> CDR1as possess >70 binding sites for miR-7.<sup>14,15</sup> CDR1as was suggested to sponge miR-7 and thereby prevent suppression of miR-7 targets.<sup>14</sup> CDR1as was also shown to act as a post-transcriptional regulator of miR-7 availability in the human brain.<sup>14</sup> However, as the seed sequence of miR-7 is partially complementary to CDR1as, it does not guide miR-7 for degradation.<sup>16,17</sup> Furthermore, CDR1as loss causes miR-7 downregulation in the brain, suggesting that CDR1as does not sequester miR-7 after it attaches to its target genes; instead, CDR1as may serve as a miR-7 storehouse.<sup>16,17</sup> We previously reported that CDR1as was downregulated as early as 3 h of reperfusion following focal ischemia in mice.<sup>4</sup> We also showed that focal ischemia significantly reduces cerebral miR-7 levels, which are causally related to derepression of  $\alpha$ -synuclein ( $\alpha$ -Syn) and ischemic brain damage.<sup>18</sup>

We further showed that replenishing miR-7 with a mimic significantly alleviates post-stroke brain damage and motor/cognitive dysfunction.<sup>18,19</sup> We presently evaluated if downregulation of CDR1as promotes secondary brain damage after transient focal ischemia in mice and, if yes, by reducing miR-7 levels leading to derepression of  $\alpha$ -Syn. We overexpressed CDR1as in the cerebral cortex of adult male mice subjected to transient focal ischemia using an adeno-associated virus serotype 9 (AAV9) vector containing CDR1as sequence.<sup>14</sup>

## RESULTS

### Focal ischemia downregulated CDR1as and miR-7

Bioinformatics analysis shows that CDR1as and miR-7 sequences are highly conserved (Figure 1A). Furthermore, there is a high complementarity between CDR1as and miR-7 as well as between miR-7 and  $\alpha$ -Syn (Figure 1A). Transient middle cerebral artery occlusion (MCAO) resulted in a significant downregulation of CDR1as between

Received 8 July 2022; accepted 30 November 2022;  
<https://doi.org/10.1016/j.omtn.2022.11.022>.

**Correspondence:** Suresh L Mehta, PhD, Department of Neurological Surgery, University of Wisconsin-Madison, Mail code CSC-8660, 600 Highland Ave, Madison, WI 53792, USA.

**E-mail:** [mehta@neurosurgery.wisc.edu](mailto:mehta@neurosurgery.wisc.edu)



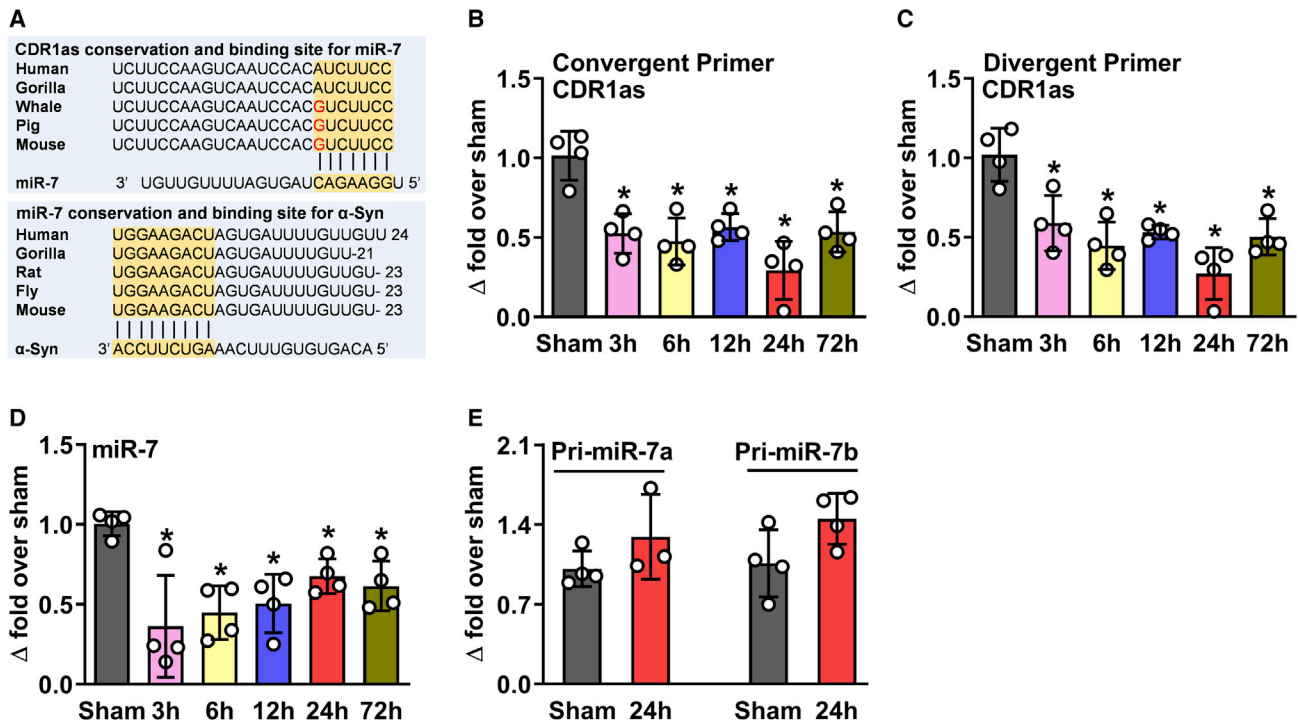


**Figure 1. Transient focal ischemia decreased CDR1as and miR-7 levels in the brain**

miR-7 and CDR1as belong to different ncRNA families; their sequences and binding sites are highly conserved across species (A). Real-time PCR analysis of CDR1as levels using convergent (B) and divergent (C) primers in the cerebral peri-infarct region of adult male mice at various time points of reperfusion following a 60-min of transient focal ischemia compared with sham mice. Mature miR-7 levels (D) but not pri-miR-7 (E) mimicked CDR1as levels in the cerebral peri-infarct region of adult male mice at various time points of reperfusion following a 1-h of transient MCAO compared with sham mice. \* $p < 0.05$  compared with the equivalent control group by Mann-Whitney U test or one-way ANOVA followed by Sidak's multiple-comparisons test; data are mean SD ( $n = 3-4$  mice per group).

3 and 72 h after reperfusion compared with sham (by 50%–70%;  $p < 0.05$ ) tested by both convergent (Figure 1B) and divergent (Figure 1C) primers. Transient MCAO also significantly decreased miR-7 levels between 3 and 72 h of reperfusion compared with sham (by 50%–64%;  $p < 0.05$ ) (Figures 1D and S1). miR-7 is transcribed mainly from two different chromosomes as primary miRNA (pri-miR-7a and pri-miR-7b) encoding the corresponding precursor sequence, which is eventually spliced into mature miR-7. The transcription of miR-7 (pri-miR-7a and pri-miR-7b) is not significantly changed (Figure 1E); still, its mature levels are considerably decreased following transient MCAO (Figure 1D). This suggests that transient MCAO affected the post-transcriptional downregulation but not the biogenesis of miR-7.

#### CDR1as AAV9 treatment increased cerebral CDR1as levels

A CDR1as expression plasmid with a CDR1as sequence (red) and HindIII and PspOMI enzyme restriction sites (Figure 2A) produced a 3,689-bp CDR1as sequence upon digestion (Figure 2B). This CDR1as insert was packaged into the AAV9 virus with upstream HindIII and downstream NotI restriction sites (Figure 2C). When mice were injected with AAV9-CDR1as, high levels of CDR1as expression ( $p < 0.05$ ) were detected by 21 days, compared with the

AAV9-Control-treated cohort observed with divergent primers (designed to span the circular junction site; 188-bp amplicon) in real-time PCR (Figure 2D). Using the AAV9-GFP, we confirmed the wide distribution of the injected AAV9 into the ipsilateral cerebral cortex 21 days after injection (Figure 2E). There were no statistically significant differences between the regional cerebral blood flow (rCBF) in AAV9-CDR1as and AAV9-Control-injected mice (Figure 2F), motor function analyzed by rotarod test (Figure S2A) and beam walk test (Figure S2B), and cognitive function analyzed by Morris water maze test (Figures S2C–S2E). Following 21 days after the injection, AAV9-CDR1as or AAV9-Control cohorts of mice were subjected to either sham or transient MCAO/24 h or 72 h reperfusion. In all three groups, CDR1as levels were observed to be distinctly higher ( $p < 0.05$ ) than AAV9-Control-treated cohort (Figure 2G). A markedly higher CDR1as expression ( $p < 0.05$ ) was also seen even at 4 months after the vector injection in mice subjected to either transient MCAO or sham (Figure 2H).

#### CDR1as overexpression increased miR-7 levels in the post-stroke brain

Transient MCAO downregulated miR-7 levels as reported before (Figures 1D and 3A).<sup>18</sup> Whereas, AAV9-CDR1as treatment

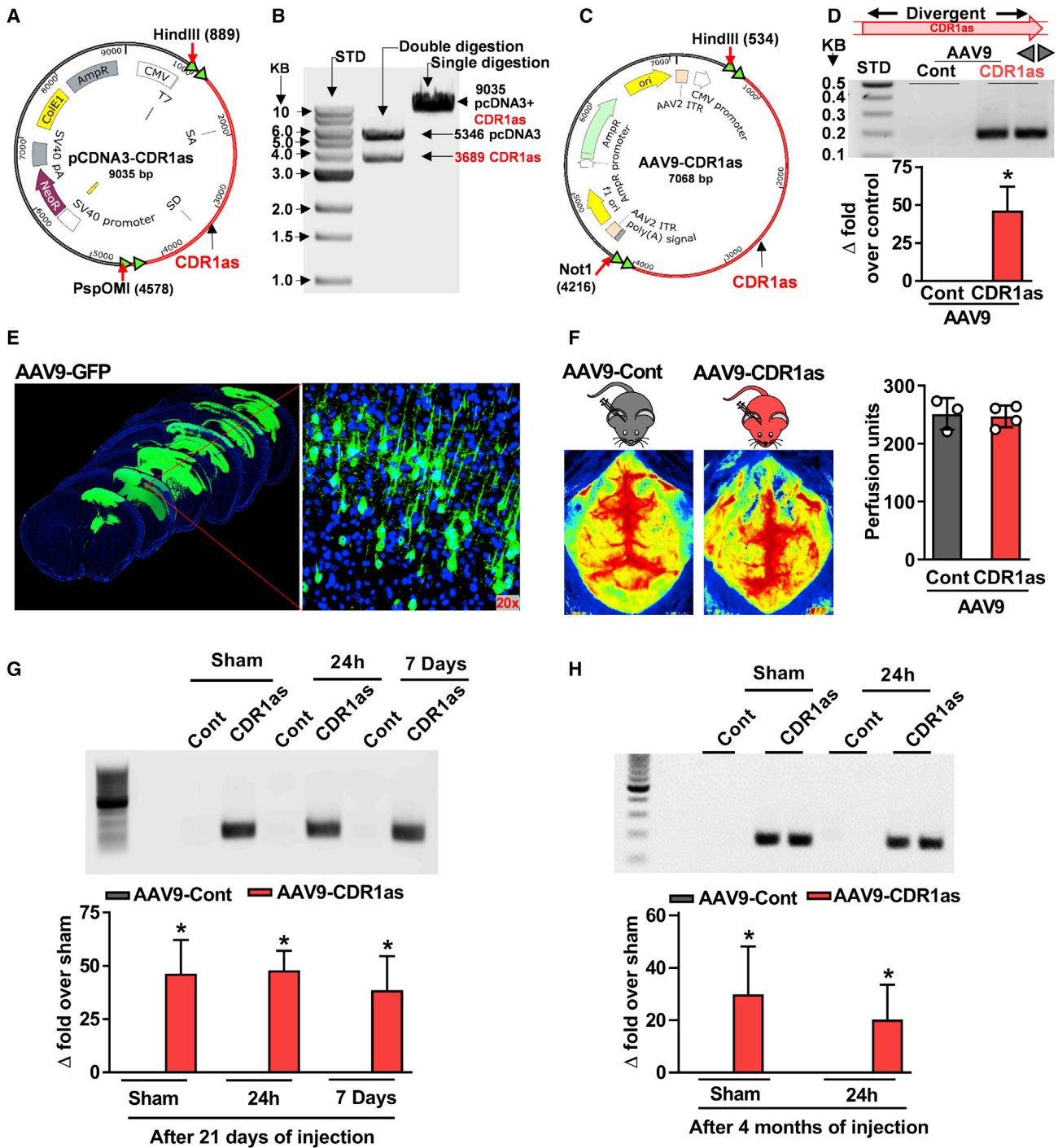


**Figure 2. CDR1as overexpression elevated CDR1as levels without affecting normal physiologic function**

CDR1as expression plasmid map with a CDR1as sequence (red) and HindIII and PspOMI enzyme restriction sites (A), digested CDR1as insert (B), and packaged into the AAV9 virus to overexpress CDR1as (C). AAV9-CDR1as treated mice showed abundant CDR1as expression with real-time PCR using divergent primers compared with AAV9-Control mice (D; n = 3–4/group). GFP distribution in the cerebral cortex at 21 days after AAV9 injection (E). Laser speckle measurement of rCBF in AAV9-CDR1as and AAV9-Control cohort (n = 3–4/group) showed no difference in rCBF between them (F). Estimation of CDR1as levels ( $\times 10^3$ ) with real-time PCR after 21 days of injection and at days 1 and 7 of reperfusion (G), and at 4 months of injection and 1 day of reperfusion (H) following 60 min of transient MCAO (n = 4/group). Cont = Control. Values are mean  $\pm$  SD. \*p < 0.05 compared with Sham with Mann-Whitney U test.



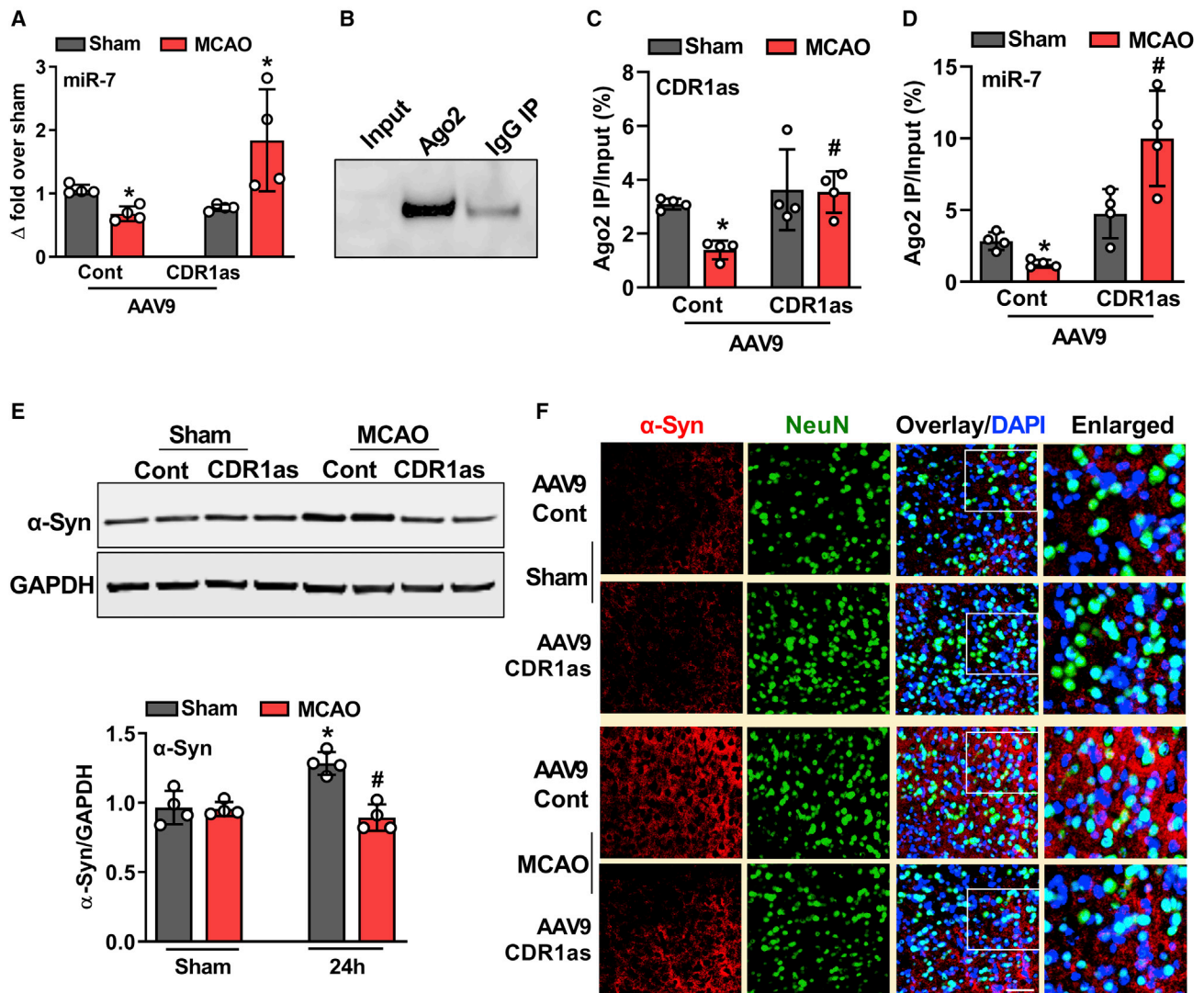


**Figure 3. CDR1as overexpression increased miR-7 enrichment and suppressed  $\alpha$ -Syn abundance**

The miR-7 levels at 1 day of reperfusion following transient MCAO in the peri-infarct cortex of the AAV9-CDR1as cohort are significantly higher than in the AAV9-Control cohort (A). The immunoprecipitated protein probed with Ago2 antibody showed robust enrichment of Ago2 protein in the pull-down fraction (B). RNA isolated from Ago-complex after RIP assay of peri-infarct cortex at day 1 of reperfusion from the AAV9-CDR1as cohort was significantly higher in CDR1as (C) and miR-7 (D) levels than AAV9-Control cohort. The  $\alpha$ -Syn protein levels in the peri-infarct cortex at 1 day of reperfusion after transient MCAO were also significantly lower in the AAV9-CDR1as cohort compared with the AAV9-Control cohort (E and F). Brain sections (40  $\mu$ m) were costained with NeuN (neuronal nuclei). Blue is DAPI for the nucleus. Cont = Control. Data are mean  $\pm$  SD (n = 4/group). \*p < 0.05 compared with sham and #p < 0.05 compared with the equivalent MCAO group by Mann-Whitney U test. Scale bar represents 50  $\mu$ m.

significantly increased cerebral miR-7 levels at 24 h of reperfusion following transient MCAO compared with the AAV9-Control-injected cohort (Figure 3A). Immunoprecipitated protein probed with Ago2 antibody showed robust enrichment of Ago2 in the pull-down fraction (Figure 3B). RNA-immunoprecipitation (RIP) analysis showed increased post-ischemic enrichment of both CDR1as and miR-7 in the AAV9-CDR1as-treated cohort at 1 day of reperfusion (Figures 3C and 3D). The results were normalized to the input to confirm that increased miR-7 in the ischemic brain is exclusively

due to CDR1as overexpression. These findings suggest that by safeguarding miR-7, CDR1as might preserve post-stroke miR-7 levels.

#### Post-ischemic $\alpha$ -Syn induction is CDR1as/miR-7 dependent

We recently showed that miR-7 directly binds to  $\alpha$ -Syn, so miR-7 downregulation derepresses  $\alpha$ -Syn translation.<sup>18,20</sup> Hence, restoring post-stroke miR-7 levels reduces  $\alpha$ -Syn protein abundance and protects the brain.<sup>18,19</sup> We currently show that AAV9-CDR1as treatment significantly suppresses the post-ischemic  $\alpha$ -Syn protein levels in the

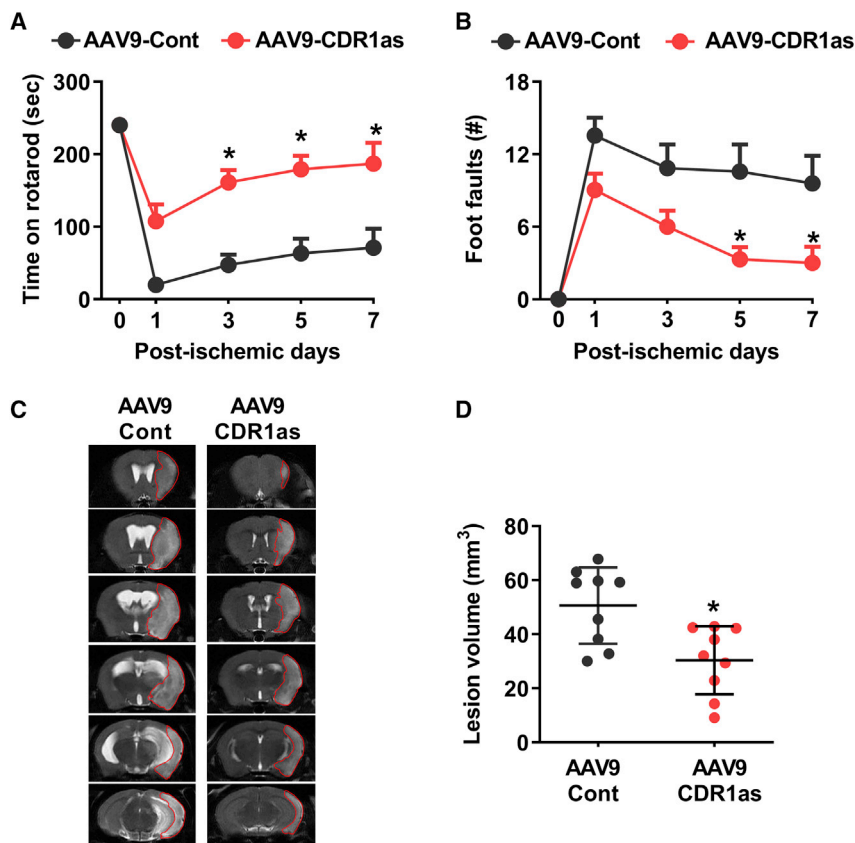


**Figure 4. CDR1as overexpression decreased neurologic deficits and infarction**

Mice injected with AAV9-CDR1as showed significantly improved post-stroke motor recovery between days 3 and 7 of reperfusion compared with AAV9-Controls studied by rotarod test (A) and beam walk test (B). Ischemic lesion detected by T2-MRI at day 7 of reperfusion (C) and the infarct volume computed with ImageJ showed significantly smaller damage in the AAV9-CDR1as cohort compared with the AAV9-Control cohort (D). Values are mean  $\pm$  SD ( $n = 9/\text{group}$ ). \* $p < 0.05$  by repeated-measures ANOVA with Bonferroni's test (motor function) or Mann-Whitney U test (lesion volume). Cont = Control.

peri-infarct cortex at 1 day of reperfusion following transient MCAO compared with the AAV9-Control-treated cohort (by 30%;  $p < 0.05$ ) (Figure 3E). Immunohistochemistry confirmed lower  $\alpha$ -Syn protein expression in NeuN<sup>+</sup> neurons in the peri-infarct cortex of the AAV9-CDR1as cohort compared with the AAV9-Control cohort at 24-h of reperfusion following transient MCAO (Figure 3F).

#### CDR1as overexpression alleviated post-stroke neurologic deficits and decreased ischemic brain damage

The AAV9-CDR1as treated cohort showed significantly improved recovery of motor function assessed by rotarod test (Figure 4A) and beam walk test (Figure 4B) between 3 and 7 days of reperfusion following transient MCAO compared with AAV9-Control-treated cohort. At 7 days of reperfusion, the infarct volume estimated by T2-MRI was significantly smaller in the AAV9-CDR1as cohort compared with the AAV9-Control cohort (by ~40%;  $p < 0.05$ ) (Figures 4C and 4D).

#### CDR1as overexpression limited the post-ischemic pathological changes

In the peri-infarct cortex of the AAV9-CDR1as treated mice, cleaved caspase-3 protein levels were significantly lower than AAV9-Control-treated mice at 24-h reperfusion following transient MCAO (Figure 5A). Immunohistochemistry showed that the decreased cleaved caspase-3 protein levels in the AAV9-CDR1as-

treated mice were in NeuN<sup>+</sup> neurons in the peri-infarct cortex of mice subjected to transient MCAO and 24 h of reperfusion (Figure 5B). This indicates reduced post-ischemic neuronal apoptosis by CDR1as overexpression. The peri-infarct cortex of the AAV9-Control-treated mice also showed activation of autophagy displayed by increased LC3 conversion and ratio of LC3-II/I, which was significantly reduced after CDR1as overexpression with AAV9-CDR1as at 24 h of reperfusion following transient MCAO (Figure 5C). Immunohistochemistry showed the punctated pattern of LC3 (LC3-I to LC3-II) that colocalized with NeuN<sup>+</sup> neurons, indicating the activation of neuronal autophagy in AAV9-Control-treated mice (Figure 5D). On the contrary, CDR1as overexpression limited the change in LC3-I to II, thereby resulting in a diffused (homogeneous) pattern (inactive) at 24 h of reperfusion following transient MCAO (Figure 5D). Stroke is also known to trigger many overlapping pathological mechanisms, including mitochondrial fragmentation and inflammation, all of which contribute to secondary brain damage.<sup>7,18,20</sup> Post-ischemic induction of mitochondrial fragmentation (pDrp1 immunostaining) is significantly decreased by CDR1as overexpression (Figure 6A). Post-ischemic induction of inflammation was evaluated by constraining IL-1 $\beta$  and Iba1 (microglia). IL-1 $\beta$ , despite being directly produced by most CNS cells, is synthesized and released by microglia following a cerebral ischemic event.<sup>21–24</sup> We found that IL-1 $\beta$  immunostaining and the number of IL-1 $\beta$ -positive microglial cells visible in the peri-infarct cortex of the AAV9-Control-treated cohort decreased in AAV9-CDR1as cohort at 1 day of reperfusion following transient MCAO (Figure 6B).

#### DISCUSSION

We presently demonstrated that the circRNA CDR1as influences the availability of mature miRNA miR-7 which controls the neurotoxic  $\alpha$ -Syn that is a promoter of ischemic secondary brain damage.<sup>17–19</sup> We showed that expression of CDR1as and mature miR-7 levels persistently decreased in the post-stroke brain between 3 and 72 h of reperfusion after transient focal ischemia. We further showed

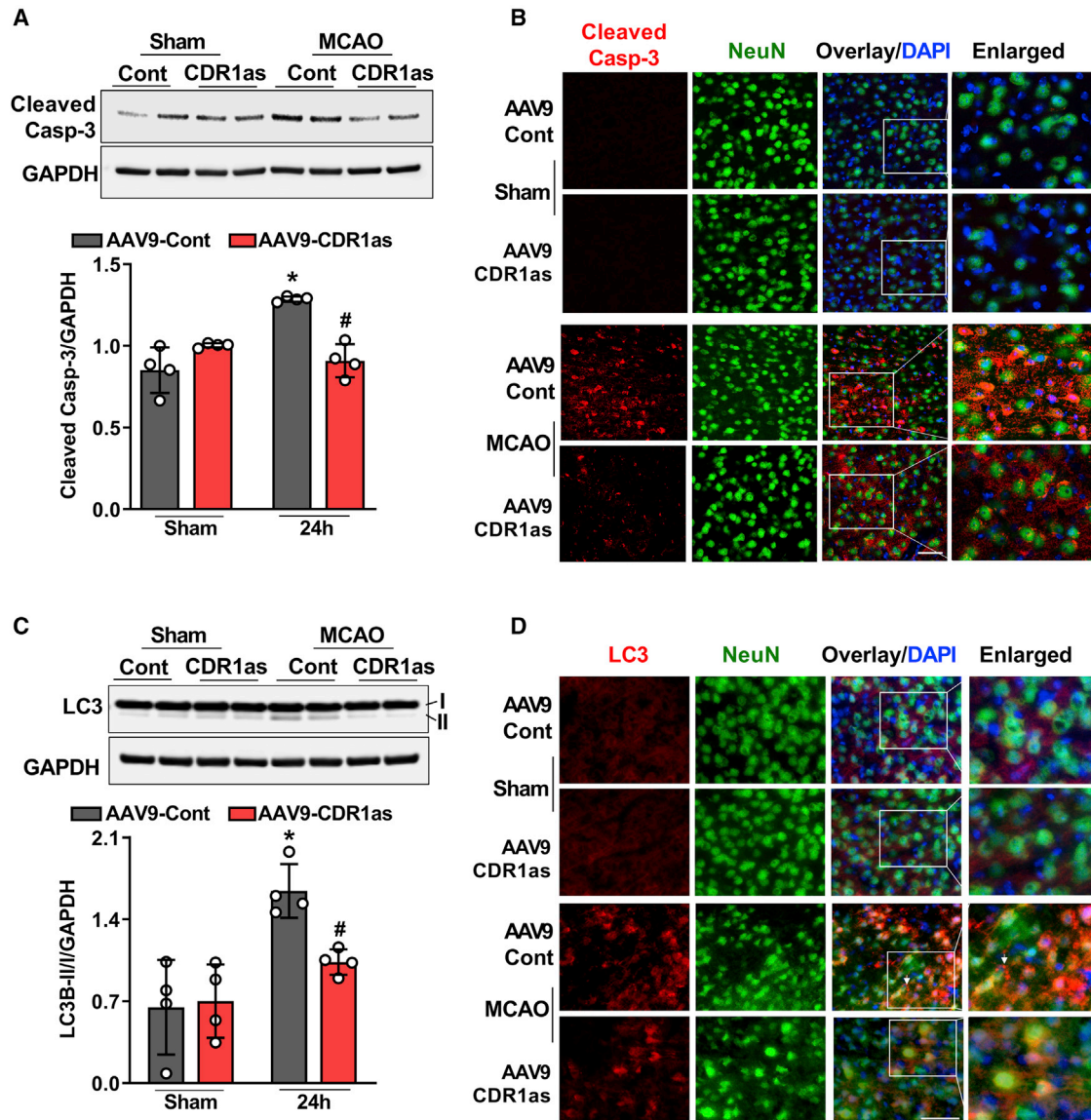


**Figure 5. CDR1as overexpression curtailed apoptosis and autophagy in the ischemic brain**

Protein abundance of a marker of apoptosis (cleaved caspase-3) in the peri-infarct area of the ipsilateral cortex from AAV9-CDR1as and AAV9-Control-injected mice, assessed at day 1 of reperfusion following 60 min of transient MCAO (A). Immunostaining of cleaved caspase-3 in the NeuN<sup>+</sup> cells (neuronal) at 1 day of reperfusion in the peri-infarct cortex of mice injected with AAV9-CDR1as and AAV9-Control (B). Autophagy marker LC3 displayed decreased LC3-I to LC3-II conversion and with LC3-II/I ratio (C) and diffused rather than punctate neuronal immunolocalization pattern (arrow) in the ischemic cortex of AAV9-CDR1as as compared with AAV9-Control cohort at day 1 of reperfusion following transient MCAO (D). Blots are representative of four independent experiments. Representative immunofluorescence images were taken from the peri-infarct region, where neurons remained relatively intact and viable. Blue is DAPI for the nucleus. Data are mean  $\pm$  SD (n = 4/group). \*p < 0.05 compared with the respective sham and #p < 0.05 compared with the respective time point group by one-way ANOVA followed by Sidak's multiple-comparisons test. Cleaved casp-3 = cleaved caspase-3 and Cont = Control. Scale bar represents 50  $\mu$ m.

that CDR1as overexpression elevated miR-7 levels and suppressed  $\alpha$ -Syn protein abundance after focal ischemia. We further showed that CDR1as overexpression decreased infarction and promoted better motor function recovery after focal ischemia. Our results also indicate that the post-ischemic neuroprotection afforded by CDR1as might be partially through curtailing apoptosis, autophagy, mito-

chondrial damage, and inflammation that aggravates ischemic brain injury.

Many studies showed that stroke alters the expression and function of different classes of ncRNAs, including miRNAs, lncRNAs, and circRNAs.<sup>1,3,4,25</sup> Studies also showed that several ncRNAs modulate



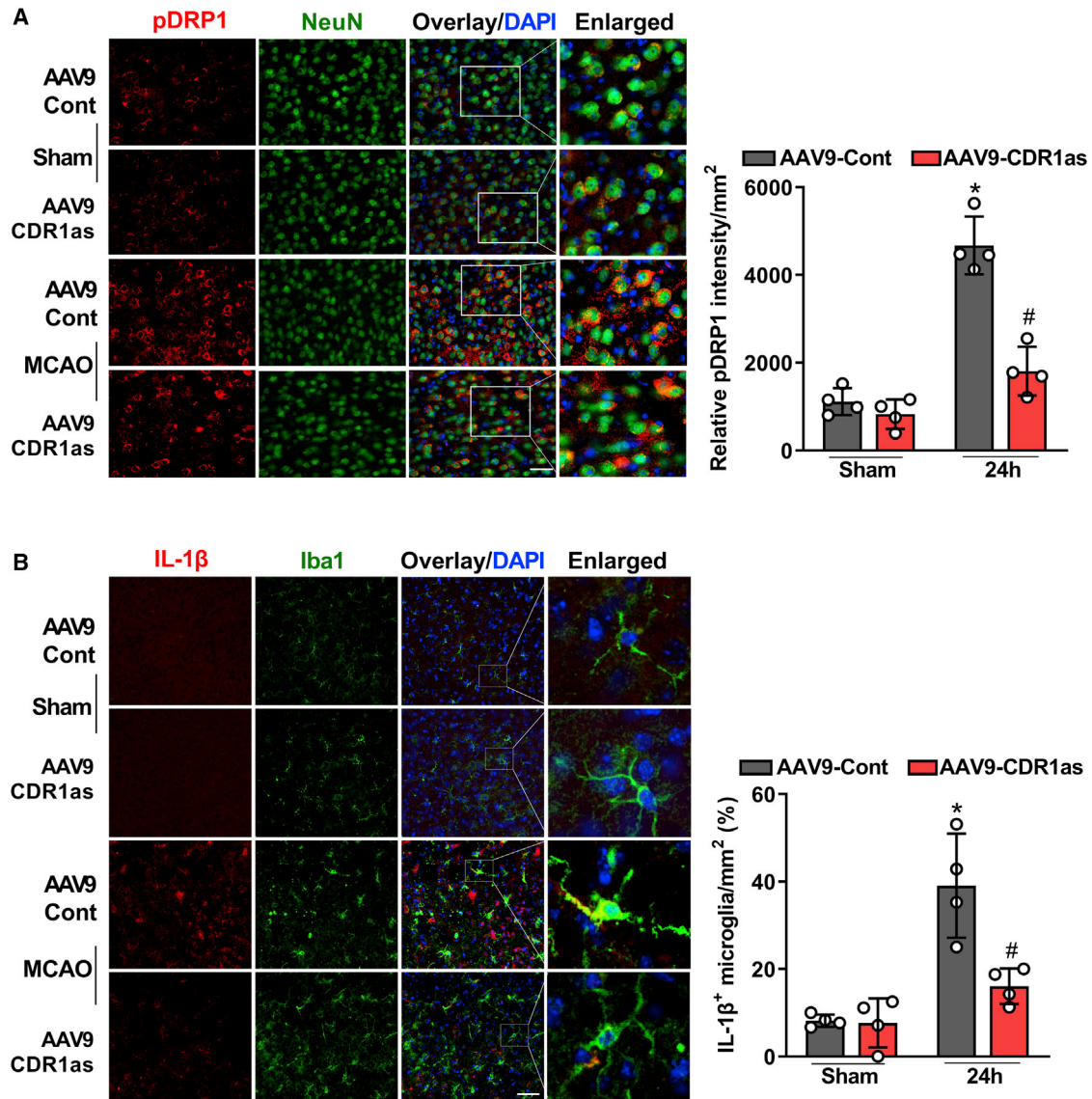


**Figure 6. CDR1as overexpression decreased pathological changes in the ischemic brain**

The immunoreactivity and quantitation of pDrp1 (a marker of mitochondrial fragmentation) in NeuN<sup>+</sup> neurons (A) and IL-1β (a marker of inflammation) in Iba1<sup>+</sup> microglia (B) in AAV9-CDR1as compared with AAV9-Controls at 1 day of reperfusion following transient MCAO (n = 4/group). \*p < 0.05 compared with the respective sham and #p < 0.05 compared with the respective time point group by one-way ANOVA followed by Sidak's multiple-comparisons test. Scale bar represents 50 μm.

post-stroke brain damage and/or recovery.<sup>7,9,18,19,26,27</sup> Furthermore, various classes of ncRNAs are known to collaborate and regulate each other.<sup>8,13,14,28</sup> Hence, understanding the dynamics and association of ncRNAs after stroke is essential to design effective therapies.

We recently showed that focal ischemia significantly reduces the levels of the prosurvival miRNA miR-7, which is highly abundant in the brain.<sup>18,19,29</sup> The miR-7 knockout mice showed increased sensitization to ischemic neural damage and worsened motor dysfunction, whereas treatment with a miR-7 mimic promoted post-stroke recov-

ery.<sup>18,19</sup> Parallel studies from our lab showed that induction of α-Syn protein expression is a major inducer of ischemic brain damage, and the neuroprotection afforded by miR-7 is due to its ability to repress α-Syn translation.<sup>18,20</sup> However, the mechanisms that are responsible for decreased miR-7 levels in the post-stroke brain are not well-understood. Hence, we tested if stroke downregulates the miR-7 transcription. However, the present studies showed that neither pri-miR-7a nor pri-miR-7b levels were unaltered in the mouse brain following transient MCAO. This indicates the possibility of post-transcriptional regulation of miR-7 levels after stroke.

Several mature miRNAs have tissue-specific expression patterns, even though that may not be the case with their corresponding primary transcripts.<sup>30</sup> Other mechanisms like Musashi homolog 2 (MSI2) and Hu antigen R (HuR) proteins are known to inhibit miR-7 processing and thus regulate mature miR-7 levels.<sup>30</sup> However, we observed that mature miR-7, but not its primary transcripts, is downregulated in the post-stroke brain, indicating that these mechanisms might not be responsible for the decreased abundance of miR-7 in the post-stroke brain. In mammals, miR-7 is formed from intron 15 of the heterogeneous nuclear ribonucleic protein K (hnRNP K) gene and is predominately enriched in the brain. Intriguingly, this gene transcribes and forms a hnRNP K protein in most organs.<sup>30</sup> This disparity indicates that miR-7 expression is regulated at the post-transcriptional level.<sup>17</sup>

We then tested if miR-7 is controlled post-transcriptionally in the ischemic brain. The circRNA CDR1as contains >70 miR-7 binding sites and is thought to act as a miR-7 sponge.<sup>13,14,17</sup> Functionally, CDR1as might act as a reservoir that protects miR-7 from the degradation by endonucleases and can transport and release miR-7 as needed.<sup>17</sup> The present study showed that focal ischemia leads to the downregulation of CDR1as in the mouse brain, which might increase the accessibility of miR-7 for degradation. To support this notion, we replenished CDR1as by transfecting the mouse brain with an AAV9-CDR1as. This increased the CDR1as levels without inducing any toxicity. Furthermore, AAV9-CDR1as-treated mice showed increased miR-7 levels, significantly curtailed ischemic brain damage and better recovery of post-ischemic motor function. CDR1as overexpression also decreased neuronal apoptosis, autophagy, mitochondrial fragmentation, and inflammation in the post-stroke brain. Notably, both miR-7 and CDR1as are known to be primarily expressed in neurons with little expression in non-neuronal cells.<sup>17</sup>

Importantly, CDR1as levels persisted even 4 months after the AAV9 treatment, and CDR1as overexpression beyond physiologic levels did not cause neurologic impairment or mortality. Although miR-7 binding sites on CDR1as are highly conserved, they lack significant complementarity beyond the seed region, implying that miR-7 can stably bind to CDR1as, and the CDR1as-miR-7 complex is unlikely degraded by RNA-induced silencing complex containing Ago2.<sup>17</sup> Furthermore, miR-7 binding to CDR1as results in forming a unique complex with three distinct structural domains: two short helices with an internal loop, the hinge, and the triple-helix, which results in the circularization of CDR1as.<sup>27</sup>

Previous studies also suggest that CDR1as deficiency leads to the downregulation of miR-7 in neural tissues.<sup>17</sup> In agreement, we noticed that a sustained decline in CDR1as levels led to an extended decrease of miR-7 in the post-stroke brain. A recent study reported that miR-7 (downregulated) and miR-671 (upregulated) that directly interact with CDR1as are the only miRNAs altered in the CDR1as-deficient mice.<sup>17</sup> Although the mechanisms responsible for CDR1as downregulation in the post-stroke brain are not clear; evidence suggests that miR-671, which contains the same seed sequence as

miR-7, but with extended complementarity, forms an almost perfect double helix with CDR1as and directs Ago2-slicer-dependent cleavage of CDR1as.<sup>13,17,31</sup> It is proposed that miR-671 might aid CDR1as in releasing miR-7 under certain conditions, but this needs to be confirmed by future studies.<sup>17</sup>

Nevertheless, we observed that CDR1as overexpression resulted in elevated miR-7 and suppression of miR-7 target  $\alpha$ -Syn following transient focal ischemia, suggesting that CDR1as may not sequester miR-7 once it binds to its target genes.<sup>16</sup> Additionally, recent observation of a negative correlation between CDR1as and several miR-7 targets such as PAK1 and CDK1 argues against sequestering miR-7 from its target genes by CDR1as.<sup>16</sup> Hence, besides serving as a repository, CDR1as might be involved in stability, intracellular trafficking, and timed release of miR-7.<sup>13,17</sup> Moreover, miR-7 aids in CDR1as circularization and stability, whereas once formed, CDR1as shields miR-7 from degradation, which strongly favors the reshaping of miRNA sponge theory.<sup>13,17</sup>

We and others have shown that miR-7 regulates the abundance of  $\alpha$ -Syn in the brain.<sup>18,19,32</sup> The normal cellular functions of  $\alpha$ -Syn are still not clear. But, its induction, accumulation, and/or aggregation can cause neurodegeneration and neuropathology; for example, the acute post-stroke  $\alpha$ -Syn induction and/or aggregation aggravates ischemic brain damage.<sup>20,32,33</sup> Stroke is known to cause varying degrees of neuronal injury that impairs sensorimotor and cognitive brain functions in both males and females.<sup>7,9,18,20,26,34</sup> The present study used only adult mice to mechanistically show that CDR1as overexpression increases miR-7 levels and suppresses  $\alpha$ -Syn induction. Aging and co-morbidities significantly impact the incidence of stroke and its consequences.<sup>35</sup> They also influence the efficacy of therapies. However, not testing aged and co-morbid mice is a limitation of the present study. We previously showed that ischemic brain damage could be reduced regardless of age by limiting the  $\alpha$ -Syn induction and restoring miR-7 basal levels.<sup>18</sup> Nevertheless, additional studies are needed to confirm whether CDR1as overexpression elevates miR-7 basal levels and prevents ischemic brain damage, irrespective of age or co-morbid conditions. Recent studies showed significant motor deficits and neuronal deposits of pathologic  $\alpha$ -Syn throughout the brain that deteriorate over time between 180 and 360 days after ischemia in  $\alpha$ -Syn overexpressing mice.<sup>33</sup> This is further supported by evidence indicating that deregulation of miR-7 in mice lacking CDR1as locus resulted in synaptic malfunction and a deficit in pre-pulse inhibition of the startle reflex.<sup>17</sup>

We used AAV9 pre-stroke as a tool to overexpress CDR1as to delineate the mechanistic connection between CDR1as and miR-7. A similar AAV-mediated gene therapy has already been tested in humans and approved by US Food and Drug Administration mainly to correct biallelic mutations in the survival motor neuron 1 (SMN1) gene that causes spinal muscular atrophy and correct a biallelic RPE65 mutation in patients with retinal dystrophy.<sup>36,37</sup> Evidence also points to viral vector-mediated gene therapy as a potential stroke treatment by expressing genes that alter the post-ischemic



pathophysiological progression.<sup>38</sup> A recent study reported converting proliferative astrocytes in the neocortex of young and old mice following cerebral ischemia by utilizing a retroviral delivery system encoding the transcription factor Ngn2 alone or in conjunction with the anti-apoptotic protein Bcl-2.<sup>39</sup> However, additional research is required to validate the clinical use of such strategies for the treatment of stroke, including the non-invasive technique of delivering viral vectors and the optimization of the target, dose, and viability. Although the AAV9-based pretreatment strategy cannot be therapeutic, particularly in stroke, pretreatment/preconditioning is proven to reduce the incidence and consequences of vascular diseases. Indeed, preconditioning is crucial in curtailing the severity of ischemic brain injury after the onset and also helps to prevent recurrent strokes.

Besides overexpression, the biggest challenge of circRNAs is circularization *in vivo*. To overcome such a roadblock, Hanson et al. inverted a portion of the upstream sequence of CDR1as and inserted it downstream to help with effective circularization.<sup>14</sup> Using this approach, we achieved efficient induction/circularization of CDR1as in the mouse brain. Moreover, CDR1as can be packaged in the extracellular vesicles (EVs) and/or liposomes and can be delivered *in vivo* (IV) to increase the translation potential. Although we will test this in future studies, Yang and colleagues recently validated a similar RNA drug delivery approach to administer circRNA circSCMH1 (IV) post-stroke using EVs to target functional recovery in both mice and monkeys.<sup>40</sup> Overall, the current finding implies that targeting circRNA CDR1as is a novel therapeutic strategy to efficiently control miR-7/ $\alpha$ -Syn to minimize post-stroke brain damage.

## MATERIALS AND METHODS

The University of Wisconsin Research Animal Resources and Care Committee approved all experimental protocols using animals. Experiments were conducted in compliance with the “Animal Research: Reporting of In Vivo Experiments (ARRIVE)” guidelines, and care was in accordance with the Guide for the Care and Use of Laboratory Animals, US Department of Health and Human Services Publication Number 86-23 (revised).<sup>41</sup> Animals were divided randomly into groups, and the outcome measures were evaluated blindly.

### Focal ischemia

A 1-h transient intraluminal middle cerebral artery occlusion (MCAO) was conducted in adult male C57BL/6J mice (12 weeks, 27 ± 2 g, Charles River, USA) under isoflurane anesthesia with 6-0 silicon-coated monofilament (Doccol, USA), followed by 1–7 days of reperfusion.<sup>4,18–20,34,41</sup> Sham-operated animals received a similar surgical procedure without MCAO. Regional cerebral blood flow (rCBF) and physiological parameters (pH, PaO<sub>2</sub>, PaCO<sub>2</sub>, hemoglobin, and blood glucose) were monitored, and body temperature was maintained at 37.0°C ± 0.5°C during surgery. Mice with no signs of neurologic deficits during reperfusion or signs of hemorrhage during imaging or after euthanasia were excluded. The rCBF was estimated by laser speckle imaging (PeriCam PSI HR System; Perimed, USA) to confirm occlusion and reperfusion under isoflurane anesthesia in mice subjected to transient MCAO.<sup>18</sup> The rCBF was measured in

the ipsilateral side of the brain that was injected with control or CDR1as overexpressing vector. The total rCBF in the selected region of interest was expressed as arbitrary perfusion units and compared among the groups tested.<sup>18</sup>

### CDR1as overexpression

A pCDNA3-CDR1as plasmid containing invert repeat flanking introns for circular CDR1as and restriction digestion sites was amplified in *E. coli* grown on the agar plates with ampicillin selection, digested with HindIII and PspOMI restriction enzymes, and CDR1as fragment was ligated to HindIII and NotI (compatible to PspOMI site) restriction digestion sites and packaged into recombinant AAV9.<sup>14</sup> The AAV9-CDR1as vector was amplified, purified, and titrated for *in vivo* studies (Vector Biolabs, USA).<sup>42,43</sup> Cohorts of adult, male C57BL/6 mice were stereotaxically injected into the cerebral cortex (from bregma: 0.25 mm posterior, 1.5 mm ventral, and 3 mm lateral) with either AAV9-CDR1as (2  $\mu$ L; 10<sup>13</sup> genome copies/ml) or AAV9-Control (null)/GFP. CDR1as levels were estimated in the cortical tissue by real-time PCR after 21 days of injection.

### Motor function and infarct volume assessment

Post-ischemic motor learning, balance, and coordination were evaluated with a rotarod test (4 min on a cylinder rotating at 8 RPM) and beam walk test (number of foot faults while crossing a 120-cm-long beam) on days 1, 3, 5, and 7 of reperfusion following transient MCAO as described previously.<sup>7,9,18,19,34</sup> Mice were pre-trained for 3 days before the induction of ischemia. Infarct size was assessed at 7 days of reperfusion with T2-MRI (4.7T small animal system scanner; Agilent Technologies, USA).<sup>34</sup> Briefly, mice were anesthetized with isoflurane and scanned up to 8–10 coronal brain slices at 1.0 mm thickness and 20 × 20 mm<sup>2</sup> fields of view. The respiration rate and distress were monitored during the imaging. Infarct size was measured blindly using NIH ImageJ software with an FDF plugin.<sup>19</sup> Infarct volume was computed by numeric integration of data from serial coronal sections to sectional intervals and corrected for edema as described before.<sup>9,18,19,34</sup>

### RNA-immunoprecipitation

The interaction of CDR1as with miR-7 was analyzed using Magna RIP (Millipore Sigma, USA). Total RNA isolated from the ipsilateral peri-infarct cortex of AAV9-CDR1as- and AAV9-Control-injected mice subjected to transient MCAO/24 h of reperfusion and sham surgery was immunoprecipitated using Ago2 antibody (RIP Grade; Diagenode, USA). The Ago2 protein and Ago-complex containing pull-down fraction of RNAs (CDR1as and miR-7) were extracted and analyzed with western blotting and real-time PCR, respectively.

### Real-time PCR

CDR1as and miR-7 levels were estimated by real-time PCR using the SYBR-green method as described earlier.<sup>4,7,18</sup> The comparative threshold cycle (Ct) method ( $2^{-\Delta\Delta Ct}$ ) was used to compute the relative expression after normalizing the changes with 18S rRNA. CDR1as was amplified using both convergent (5'-CTCCACATCTTCCAGCATCTT-3' and 5'-GATACGGCAGACACCAGAAA-3')

and divergent (5'-ATGTTGGAAGACCTTGGTACTGGC-3' and 5'-CCAACATCTCCACATCTTCCAGCA-3' and for overexpression 5'-AGACCTTGAGATTATTGGAAGACTTGA-3' and 5'-TACCCA GTCTTCCATCAACTGGCT-3') primers.<sup>4</sup> The primers used for miR-7 were 5'-GTTGGCCTAGTTCTGTGTGGA-3' and 5'-TAGAG GTGGCCTGTGCCATA-3'.

### Western blotting

In brief, protein extracts from the peri-infarct cortex were electrophoresed, blotted onto nitrocellulose membranes, and probed with antibodies against  $\alpha$ -Syn (Cell Signaling Technology; Cat#: 2642S; 1:1,000) cleaved caspase-3 (Cell Signaling Technology; Cat#: 9661S; 1:1,000), Ago2 (Diagenode; Cat#: C15200167-100; 1:500), LC3 (Cell Signaling Technology; Cat#: 12741S; 1:1,000), and GAPDH (Cell Signaling Technology; Cat#: 2118; 1:1,000) followed by HRP (Cell Signaling Technology) or IRDye Infrared Fluorescent Dyes (LI-COR) conjugated anti-rabbit or anti-mouse antibodies. Blots were developed using enhanced chemiluminescence (Life Technologies; Cat#: 34076) or scanned with a nearinfrared spectrum (between 680 and 800 nm) analyzer (Odyssey CLx, LI-COR) and quantified with Image Studio software (LI-COR Biotechnology, USA).

### Immunostaining

Brain sections (40  $\mu$ m; between the coordinates +1 to +1.5 from bregma) were immunostained with antibody against  $\alpha$ -Syn (Cell Signaling Technology; Cat#: 4179S; 1:200), cleaved caspase-3 (Cell Signaling Technology; Cat#: 9661S; 1:500), LC3 (Cell Signaling Technology; Cat#: 12741S; 1:200), pDrp-1 (Cell Signaling Technology; Cat#: 3455S; 1:400), and IL-1 $\beta$  (Cell Signaling Technology; Cat#: 12741S; 1:100) and costained with either NeuN (Millipore; Cat#: MAB377; 1:300) or Iba1 (CST; Cat#: 17198S; 1:200) as described earlier.<sup>18,19,31</sup> An investigator blinded to the study groups microscopically analyzed the immunostaining as described before.<sup>7,18,19</sup>

### Statistical analysis

Mann-Whitney U test was used to compare two groups, and one-way ANOVA followed by Sidak's multiple-comparisons test was used to compare multiple groups. Two-way repeated-measures ANOVA with Bonferroni's test was used to analyze data from the same subjects at different time points.

### DATA AND MATERIALS AVAILABILITY

All data needed to evaluate the conclusions in the paper are present in the main document or the [supplemental information](#).

### SUPPLEMENTAL INFORMATION

Supplemental information can be found online at <https://doi.org/10.1016/j.omtn.2022.11.022>.

### ACKNOWLEDGMENTS

This work was partially supported by UW ICTR 233AAH1544, NIH RO1 NS109459, and UW Department of Neurological Surgery. Dr. Vemuganti is the recipient of a Research Career Scientist award (# IK6BX005690) from the US Department of Veterans Affairs. We

thank Dr. Thomas Birkballe Hansen, PhD, Aarhus University, Denmark, for providing the pcDNA3-ciRS-7 expression plasmid.

### AUTHOR CONTRIBUTIONS

S.L.M. and R.V. contributed to the conception and design of the study; S.L.M., A.K.C., S.B., V.A., and B.C. contributed to the acquisition and analysis of data; S.L.M. and R.V. contributed to drafting the text.

### DECLARATION OF INTERESTS

The authors declare that they have no competing interests.

### REFERENCES

- Dharap, A., Bowen, K., Place, R., Li, L.C., and Vemuganti, R. (2009). Transient focal ischemia induces extensive temporal changes in rat cerebral microRNAome. *J. Cereb. Blood Flow Metab.* 29, 675–687.
- Dharap, A., Nakka, V.P., and Vemuganti, R. (2011). Altered expression of PIWI RNA in the rat brain after transient focal ischemia. *Stroke* 42, 1105–1109.
- Dharap, A., Nakka, V.P., and Vemuganti, R. (2012). Effect of focal ischemia on long noncoding RNAs. *Stroke* 43, 2800–2802.
- Mehta, S.L., Pandi, G., and Vemuganti, R. (2017). Circular RNA expression profiles alter significantly in mouse brain after transient focal ischemia. *Stroke* 48, 2541–2548.
- Dharap, A., Pokrzywa, C., Murali, S., Pandi, G., and Vemuganti, R. (2013). MicroRNA miR-324-3p induces promoter-mediated expression of RelA gene. *PLoS One* 8, e79467.
- Dharap, A., Pokrzywa, C., and Vemuganti, R. (2013). Increased binding of stroke-induced long non-coding RNAs to the transcriptional corepressors Sin3A and coREST. *ASN neuro* 5, 283–289.
- Mehta, S.L., Chokkalla, A.K., Kim, T., Bathula, S., Chelluboina, B., Morris-Blanco, K.C., Holmes, A., Banerjee, A., Chauhan, A., Lee, J., et al. (2021). Long noncoding RNA fos downstream transcript is developmentally dispensable but vital for shaping the poststroke functional outcome. *Stroke* 52, 2381–2392.
- Mehta, S.L., Dempsey, R.J., and Vemuganti, R. (2020). Role of circular RNAs in brain development and CNS diseases. *Prog. Neurobiol.* 186, 101746.
- Mehta, S.L., Kim, T., and Vemuganti, R. (2015). Long noncoding RNA FosDT promotes ischemic brain injury by interacting with REST-associated chromatin-modifying proteins. *J. Neurosci.* 35, 16443–16449.
- Pandi, G., Nakka, V.P., Dharap, A., Roopra, A., and Vemuganti, R. (2013). MicroRNA miR-29c down-regulation leading to de-repression of its target DNA methyltransferase 3a promotes ischemic brain damage. *PLoS One* 8, e58039.
- Salmena, L., Poliseno, L., Tay, Y., Kats, L., and Pandolfi, P.P. (2011). A ceRNA hypothesis: the Rosetta Stone of a hidden RNA language? *Cell* 146, 353–358.
- Tay, Y., Rinn, J., and Pandolfi, P.P. (2014). The multilayered complexity of ceRNA crosstalk and competition. *Nature* 505, 344–352.
- Kleaveland, B., Shi, C.Y., Stefano, J., and Bartel, D.P. (2018). A network of noncoding regulatory RNAs acts in the mammalian brain. *Cell* 174, 350–362.e17.
- Hansen, T.B., Jensen, T.I., Clausen, B.H., Bramsen, J.B., Finsen, B., Damgaard, C.K., and Kjems, J. (2013). Natural RNA circles function as efficient microRNA sponges. *Nature* 495, 384–388.
- Memczak, S., Jens, M., Elefsinioti, A., Torti, F., Krueger, J., Rybak, A., Maier, L., Mackowiak, S.D., Gregersen, L.H., Munschauer, M., et al. (2013). Circular RNAs are a large class of animal RNAs with regulatory potency. *Nature* 495, 333–338.
- Kristensen, L.S., Ebbesen, K.K., Sokol, M., Jakobsen, T., Korsgaard, U., Eriksen, A.C., Hansen, T.B., Kjems, J., and Hager, H. (2020). Spatial expression analyses of the putative oncogene ciRS-7 in cancer reshape the microRNA sponge theory. *Nat. Commun.* 11, 4551.
- Piwecka, M., Glažar, P., Hernandez-Miranda, L.R., Memczak, S., Wolf, S.A., Rybak-Wolf, A., Filipchuk, A., Klironomos, F., Cerda Jara, C.A., Fenske, P., et al. (2017). Loss

- of a mammalian circular RNA locus causes miRNA deregulation and affects brain function. *Science* 357, eaam8526.
18. Kim, T., Mehta, S.L., Morris-Blanco, K.C., Chokkalla, A.K., Chelluboina, B., Lopez, M., Sullivan, R., Kim, H.T., Cook, T.D., Kim, J.Y., et al. (2018). The microRNA miR-7a-5p ameliorates ischemic brain damage by repressing  $\alpha$ -synuclein. *Sci. Signal.* 11, eaat4285.
  19. Mehta, S.L., Chokkalla, A.K., Bathula, S., and Vemuganti, R. (2022). MicroRNA miR-7 is essential for post-stroke functional recovery. *Transl. Stroke Res.* <https://doi.org/10.1007/s12975-021-00981-7>.
  20. Kim, T., Mehta, S.L., Kaimal, B., Lyons, K., Dempsey, R.J., and Vemuganti, R. (2016). Poststroke induction of  $\alpha$ -synuclein mediates ischemic brain damage. *J. Neurosci.* 36, 7055–7065.
  21. Luheshi, N.M., Kovács, K.J., Lopez-Castejon, G., Brough, D., and Denes, A. (2011). Interleukin-1 $\alpha$  expression precedes IL-1 $\beta$  after ischemic brain injury and is localised to areas of focal neuronal loss and penumbral tissues. *J. Neuroinflammation* 8, 186.
  22. Zhang, W., Smith, C., Howlett, C., and Stanimirovic, D. (2000). Inflammatory activation of human brain endothelial cells by hypoxic astrocytes in vitro is mediated by IL-1beta. *J. Cereb. Blood Flow Metab.* 20, 967–978.
  23. Pearson, V.L., Rothwell, N.J., and Toulmond, S. (1999). Excitotoxic brain damage in the rat induces interleukin-1beta protein in microglia and astrocytes: correlation with the progression of cell death. *Glia* 25, 311–323.
  24. Boutin, H., LeFeuvre, R.A., Horai, R., Asano, M., Iwakura, Y., and Rothwell, N.J. (2001). Role of IL-1alpha and IL-1beta in ischemic brain damage. *J. Neurosci.* 21, 5528–5534.
  25. Bhattarai, S., Pontarelli, F., Prendergast, E., and Dharap, A. (2017). Discovery of novel stroke-responsive lncRNAs in the mouse cortex using genome-wide RNA-seq. *Neurobiol. Dis.* 108, 204–212.
  26. Lopez, M.S., Morris-Blanco, K.C., Ly, N., Maves, C., Dempsey, R.J., and Vemuganti, R. (2022). MicroRNA miR-21 decreases post-stroke brain damage in rodents. *Transl. Stroke Res.* 13, 483–493.
  27. Zhang, X., Tang, X., Liu, K., Hamblin, M.H., and Yin, K.J. (2017). Long noncoding RNA Malat1 regulates cerebrovascular pathologies in ischemic stroke. *J. Neurosci.* 37, 1797–1806.
  28. Mehta, S.L., Chokkalla, A.K., and Vemuganti, R. (2021). Noncoding RNA crosstalk in brain health and diseases. *Neurochem. Int.* 149, 105139.
  29. Zhao, J., Zhou, Y., Guo, M., Yue, D., Chen, C., Liang, G., and Xu, L. (2020). MicroRNA-7: expression and function in brain physiological and pathological processes. *Cell Biosci.* 10, 77.
  30. Choudhury, N.R., de Lima Alves, F., de Andrés-Aguayo, L., Graf, T., Cáceres, J.F., Rappalber, J., and Michlewski, G. (2013). Tissue-specific control of brain-enriched miR-7 biogenesis. *Genes Dev.* 27, 24–38.
  31. Belter, A., Popenda, M., Sajek, M., Woźniak, T., Naskręt-Barciszewska, M.Z., Szachniuk, M., Jurga, S., and Barciszewski, J. (2022). A new molecular mechanism of RNA circularization and the microRNA sponge formation. *J. Biomol. Struct. Dyn.* 40, 3038–3045.
  32. Junn, E., Lee, K.W., Jeong, B.S., Chan, T.W., Im, J.Y., and Mouradian, M.M. (2009). Repression of alpha-synuclein expression and toxicity by microRNA-7. *Proc. Natl. Acad. Sci. USA* 106, 13052–13057.
  33. Lohmann, S., Grigoletto, J., Bernis, M.E., Pesch, V., Ma, L., Reithofer, S., and Tamgüney, G. (2022). Ischemic stroke causes Parkinson's disease-like pathology and symptoms in transgenic mice overexpressing alpha-synuclein. *Acta Neuropathol. Commun.* 10, 26.
  34. Chelluboina, B., Chokkalla, A.K., Mehta, S.L., Morris-Blanco, K.C., Bathula, S., Sankar, S., Park, J.S., and Vemuganti, R. (2022). Tenascin-C induction exacerbates post-stroke brain damage. *J. Cereb. Blood Flow Metab.* 42, 253–263.
  35. Candelario-Jalil, E., and Paul, S. (2021). Impact of aging and comorbidities on ischemic stroke outcomes in preclinical animal models: a translational perspective. *Exp. Neurol.* 335, 113494.
  36. Keeler, A.M., and Flotte, T.R. (2019). Recombinant adeno-associated virus gene therapy in light of luxturna (and zolgensma and glybera): where are we, and how did we get here? *Annu. Rev. Virol.* 6, 601–621.
  37. Domenger, C., and Grimm, D. (2019). Next-generation AAV vectors-do not judge a virus (only) by its cover. *Hum. Mol. Genet.* 28, R3–R14.
  38. Skukan, L., Brezak, M., Ister, R., Klimaschewski, L., Vojta, A., Zoldoš, V., and Gajović, S. (2022). Lentivirus- or AAV-mediated gene therapy interventions in ischemic stroke: a systematic review of preclinical in vivo studies. *J. Cereb. Blood Flow Metab.* 42, 219–236.
  39. Gresita, A., Glavan, D., Udristoiu, I., Catalin, B., Hermann, D.M., and Popa-Wagner, A. (2019). Very low efficiency of direct reprogramming of astrocytes into neurons in the brains of young and aged mice after cerebral ischemia. *Front. Aging Neurosci.* 11, 334.
  40. Yang, L., Han, B., Zhang, Z., Wang, S., Bai, Y., Zhang, Y., Tang, Y., Du, L., Xu, L., Wu, F., et al. (2020). Extracellular vesicle-mediated delivery of circular RNA SCMH1 promotes functional recovery in rodent and nonhuman primate ischemic stroke models. *Circulation* 142, 556–574.
  41. Percie du Sert, N., Hurst, V., Ahluwalia, A., Alam, S., Avey, M.T., Baker, M., Browne, W.J., Clark, A., Cuthill, I.C., Dirnagl, U., et al. (2020). The ARRIVE guidelines 2.0: updated guidelines for reporting animal research. *PLoS Biol.* 18, e3000410.
  42. Geng, H.H., Li, R., Su, Y.M., Xiao, J., Pan, M., Cai, X.X., and Ji, X.P. (2016). The circular RNA Cdr1as promotes myocardial infarction by mediating the regulation of miR-7a on its target genes expression. *PLoS One* 11, e0151753.
  43. Li, X., Zhang, Z., Jiang, H., Li, Q., Wang, R., Pan, H., Niu, Y., Liu, F., Gu, H., Fan, X., and Gao, J. (2018). Circular RNA circPVT1 promotes proliferation and invasion through sponging miR-125b and activating E2F2 signaling in non-small cell lung cancer. *Cell. Physiol. Biochem.* 51, 2324–2340.